Mechanism of generic time variability for chaotic pattern selection

Jung-Im Kim[1] and Hie-Tae Moon[1,2]
[1]*Department of Physics, Korea Advanced Institute of Science and Technology, Daeduk Science-town 305-701, Korea*
[2]*Research Department, Electronics and Telecommunications Research Institute, Daeduk Science-town 305-600, Korea*
(Received 2 October 1995)

We studied the mechanism of alternating pattern competition between α and β modes at the surface of a fluid layer that is forced vertically. We found that when chaos is realized, the β pattern develops the degeneracy β_R, β_L such that the choice between β_R and β_L, after each excitation of the α mode, becomes undeterministic. We found, however, well defined time variability for such a chaotic pattern selection, which appears generic.

PACS number(s): 05.45.+b, 05.40.+j, 47.20.Ky

Theoretically, it is well known that chaos is possible in a simple system with only three degrees of freedom [1]. Experimentally, it is now firmly established that some hydrodynamic systems, such as Rayleigh-Bénard convection or Taylor-Couette flow under suitable geometric configurations, can have the chaotic states that can be described by few-dimensional chaotic attractors [2]. Near critical regime where dynamics passes from a linear to nonlinear range, essential dynamics is often described by a few degrees of freedom. Chaotic dynamics in such a post-critical range has been under active research in recent years.

Still, one would like to understand the physical origin of the chaotic dynamics in simple physical terms. In this respect, the study done by Ciliberto and Gollub [3] is noteworthy: They reported experiments in which chaotic behavior clearly arises from a simple mechanism, competition between two modes of different spatial symmetry, say, between α and β patterns. With the same motivation, the purpose of this study is to provide a theoretical explanation for such simple experimental observations. Our analysis is based on the theoretical model for the above experiment derived by Meron and Procaccia [4]. We found that, for chaos to be realized with two different patterns, one of them needs to develop degeneracy, say, β_R and β_L, so that, after each excitation of the α pattern, the system has to choose one of the degenerate states, β_R or β_L. This pattern selection is found to be completely unpredictable in the long run. Explicit forms of the spatial patterns α, β_R, β_L, are shown, and the origin for the degeneracy as well as the mechanism for the chaotic behavior are discussed. Significantly, we found the existence of well defined time variability — which we refer to here as the "clock" for convenience — in such a chaotic pattern selection.

We start by introducing the physical system of interest and the relevant experimental results. The system is a cylindrical fluid layer in a container that is subjected to a small vertical oscillation. This system was first studied experimentally by Faraday [5], and the linear instability was explained by Benjamin and Ursell [6]. It is well known that if the driving amplitude exceeds a critical value $A_c(\nu)$, which is a function of frequency, the free surface is deformed, which can be written as a superposition of normal modes. The modes are basically the eigenmodes of the operator $\nabla_\perp^2$, where $\nabla_\perp = \partial_x\hat{x} + \partial_y\hat{y}$, and $z = 0$ is at the free surface of the fluid in the quiescent state. These modes are $(m,n) = J_m(k_{m,n}, r)e^{\imath m\theta}$, where J_m is the Bessel function of order, m, r is the radial coordinate, θ is the azimuthal coordinate, and the allowed wave number $k_{m,n}$ is determined by the boundary condition that the derivative $J'(k_{m,n}, R) = 0$, where R is the radius of the cylinder. The eigenmode amplitude develops an instability when the corresponding eigenfrequency (given by the dispersion law for capillary-gravity waves) is approximately in resonance with half the driving frequency ν, and A exceeds A_c. This parametric instability leads to standing waves in which the mode amplitude oscillates at $\frac{1}{2}\nu$.

Ciliberto and Gollub [3], in their experiment with water 1 cm in depth in the container ($R = 6.35$) mounted on the cone of a loudspeaker oscillating vertically, observed that the chaotic state in the postcritical regime is characterized simply by the competition between the (4,3) mode and the (7,2) mode at a mean frequency that is more than two orders of magnitude smaller than ν (*i.e.*, at long time scale). Synchronizing at the fast driving frequency, one can measure the slowly varying parts of the mode amplitudes. In this postcritical regime, Meron and Procaccia [4] were able to derive a set of two coupled complex equations from the infinite-dimensional hydrodynamical equations as the governing equations of motion for the experimental observations. Denoting the slowly varying parts of the (4,3) and (7,2) modes by α and β, the time dependence of α and β is given by

$$\begin{aligned}\alpha_t &= (-L_\alpha + \imath\phi_\alpha)\alpha + \imath\Gamma_1\alpha^* + \imath\Gamma_2|\alpha|^2\alpha \\ &\quad + \imath\Gamma_3|\beta|^2\alpha + \imath\Gamma_4\alpha^*\beta^2, \\ \beta_t &= (-L_\beta + \imath\phi_\beta)\beta + \imath\Delta_1\beta^* + \imath\Delta_2|\alpha|^2\beta \\ &\quad + \imath\Delta_3|\alpha|^2\beta + \imath\Delta_4\beta^*\alpha^2, \end{aligned} \tag{1}$$

where the real coefficients L_α, and L_β are the damping factors representing energy dissipation and the coefficients Γ_i, Δ_i, ϕ_α, and ϕ_β are determined from the boundary and initial conditions.

Meron and Procaccia [4], for the set of parameters chosen as $\phi_\alpha = \frac{49.449-0.5\omega}{1.555}$, $\phi_\beta = \frac{50.2256-0.5\omega}{1.555}$, $L_\alpha = L_\beta = 3.21543 \times 10^{-4}\omega$, $\Gamma_1 = 3.12918 \times 10^{-3}A\omega^2$, $\Gamma_2 = -3.21543 \times 10^{-3}\omega$, $\Gamma_3 = 5.46624 \times 10^{-2}\omega$, $\Gamma_4 = 0.$, $\Delta_1 =$

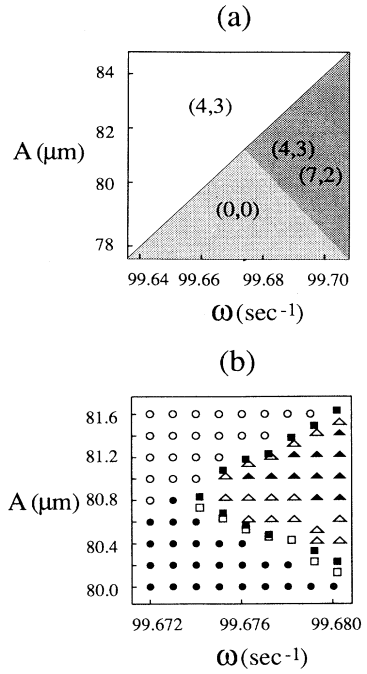

FIG. 1. (a) Phase diagram in the parameter space spanned by forcing amplitude A and frequency ω. White area, a quiescent state; shaded area; only the (4,3) mode is excited; darkened area, both the (4,3) and (7,2) modes are excited. (b) Detailed dynamical states near the center region. Each symbol stands for a dynamical state as follows. •, a quiescent state; ○, the (4,3) mode state; □, the (7,2) mode state; ■, both the (4,3) and (7,2) modes are excited but with no periodic competition. △, periodic competition between the (4,3) and (7,2) modes. ▲, chaotic competition between the (4,3) and (7,2) modes.

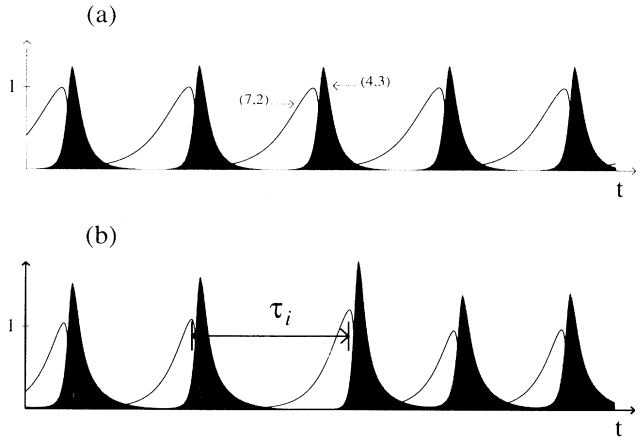

FIG. 2. Amplitude competition between the (4,3) and (7,2) modes; (a) periodic and (b) chaotic competition. The amplitudes are normalized by the time averaged amplitude of the (7,2) mode.

$3.15036 \times 10^{-3} A\omega^2$, $\Delta_2 = 4.18006 \times 10^{-3}\omega$, $\Delta_3 = \Gamma_3$, $\Delta_4 = \Gamma_4$, could basically reproduce the experimentally observed phase diagram, as shown in Fig. 1(a). The vertical axis denotes the forcing strength, and the horizontal axis stands for the forcing frequency. The region marked by (0,0) is a quiescent state with no motion, and the region marked by (4,3) stands for the region where only the (4,3) mode is excited. In the darkened region, both the (4,3) and (7,2) modes are excited and they show either periodic or chaotic competition. In Fig. 1(b), we show the detailed boundary between the two dynamical states within this darkened region. The goal of Meron and Procaccia's work [4] was to demonstrate that one can go all the way from the infinite-dimensional partial differential equations to few-dimensional chaos in a hydrodynamic system of experimental interest. The aim of this study is to have a theoretical understanding of what causes such periodic or chaotic pattern competition.

Figure 2(a) displays the time evolutions of the amplitudes of the (4,3) and (7,2) modes when they exhibit periodic competition. Here, the (7,2) mode is seen to lead the (4,3) mode by about 90°. This characteristic, as pointed out in the experiment, implies that the (7,2) mode pumps the (4,3) mode. On the other hand, Fig. 2(b) shows the chaotic competition between the two modes. Here again, it is observed that the (7,2) mode always pumps the (4,3) mode. However, the distribution of recurrence time of the (7,2) mode, denoted by τ_i in Fig. 2(b), as well as the distribution of the returning amplitudes, appear chaotic.

One may search for the reason for such observed behavior from the trajectorial motions in the phase space. Since Eq. (1) consists of two complex coupled equations, one may view the solution as a flow in a four-dimensional phase space spanned by Re(4,3), Im(4,3), Re(7,2), Im(7,2) axes. For a simple periodic motion, most of its dynamical characteristics are usually captured within a 2D phase space. So we first plotted the trajectory of the periodic state of Fig. 2(a) in the (4,3) mode subspace, i.e., the subspace spanned by Re(4,3) and Im(4,3) axes, and obtained, as a result, a circular closed orbit denoted by a, as shown in Fig. 3(a). The system is found to exhibit the bigger periodic orbit b just before it enters into the chaotic state.

Let us view the same process in the (7,2) subspace. The corresponding orbits a and b in the (7,2) mode subspace are shown in Fig. 3(b), where the dynamic evolution from a to b appears to show a marked difference from the corresponding evolution exhibited in the (4,3) mode subspace. Notice that the phase portraits that are shown here are clearly the ones for a particle moving in a double-well potential: The phase portraits indicate that between the orbit a and b exists a separatrix corresponding to the energy of the ridge in the double-well potential. The dynamical evolution from the state a to b has been known as separatrix (or homoclinic) crossings [7]. We emphasize here that one would not have noticed such separatrix crossings if the process was viewed only within the (4,3) mode subspace alone: We learned here that in the (4,3) mode subspace the orbit of the double symmetrical homoclinic loop is folded onto itself such that only one single loop appears.

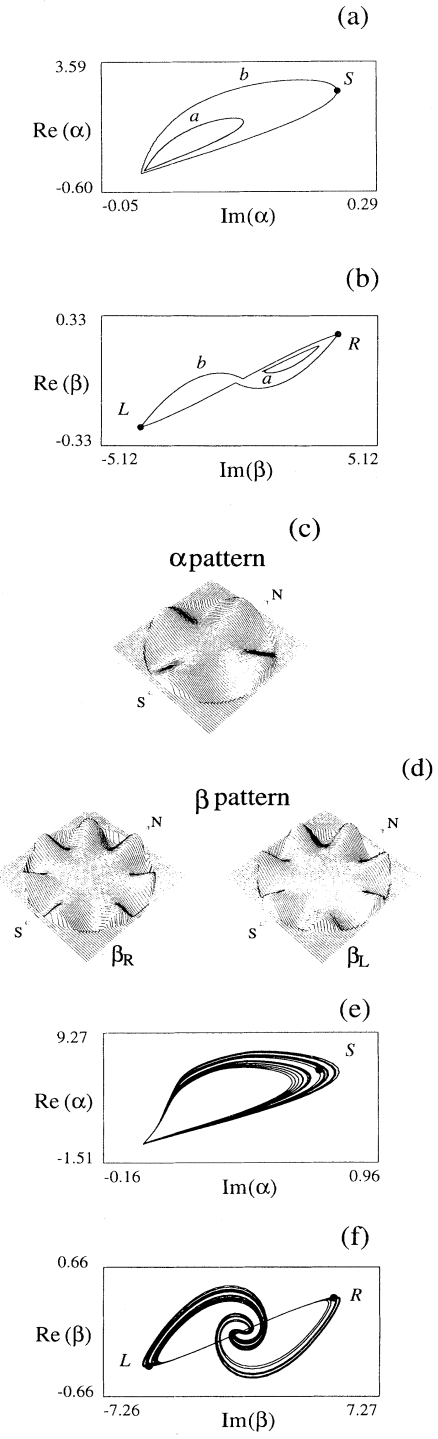

FIG. 3. Phase trajectory of the state of Fig. 2(a) projected on (a) the (4,3) mode subspace and on (b) the (7,2) mode subspace. The a orbit grows to b before losing its stability to a chaotic state. (c) Spatial pattern corresponding to the phase point S. The circle of pattern discontinuity is where the container is located. (d) The degenerate spatial patterns. β_R corresponds to the phase point R, and β_L corresponds to the phase point L. The phase trajectory of the chaotic state of Fig. 2(b) projected on (e) the (4,3) subspace and on (f) the (7,2) subspace.

The separate descriptions of the phase trajectories in the (4,3) and the (7,2) subspaces, as shown in Figs. 3(a) and 3(b), do not tell us about the relative phase relationship between the trajectories projected on each subspace. Detailed observation, however, shows that when the phase point in the (7,2) subspace reaches the farthest point away from the origin, say, the point R in the orbit b, the corresponding phase point in the (4,3) subspace is passing near the origin. And, as the phase point in the (7,2) subspace returns near to the origin from R, the corresponding phase point in the (4,3) subspace reaches the farthest point S from the origin, as shown in Fig. 3(a). As the phase point in the (7,2) subspace moves from the origin to the other farthest point L and then moves back to near the origin again, the corresponding phase point in the (4,3) space travels from S to near the origin and back to S again. The whole process mentioned above is found to repeat again and again. Thus we conclude that the phase motions in both the (4,3) and (7,2) subspaces are a "recurrent" motion bounded by a *homoclinic* orbit, and the motion in the (7,2) subspace simply leads the corresponding motion in the (4,3) subspace by $\frac{\pi}{2}$.

Next we consider the coherent patterns that are excited in the system. Notice that our system is an open system. It constantly receives energy from the outside source, i.e., from the vertical oscillation, and uses the energy to excite small length scale coherent structures where energy is dissipated away, for example, by setting up the vibrational motion of the surrounding air molecules. Notice that a point at a certain moment in the phase space represents the physical state at that moment, and we are interested in finding out the corresponding spatial pattern of the point, say, S in the (4,3) mode space. Figure 3(c) shows the spatial structure corresponding to the point S, where the circle of pattern discontinuity is where the container is located. It has four radiating arms, which we refer to here as an α pattern. Figure 3(d) shows two other spatial structures called β_R and β_L corresponding, respectively, to the points R and L in Fig. 3(b). β_R and β_L have the same spatial symmetry with seven radiating arms; rotating one by $\frac{360^\circ}{7}$ will lead to itself. Here β_R is found rotated with respect to β_L only by $\frac{360^\circ}{(7\times 2)}$ and we may thus consider these two structures as degenerate structures. These are the coherent patterns involved in the periodic competition between the (4,3) and (7,2) modes. The a state exhibits the pattern competition showing the sequence of α, β_R, α, β_R, α, β_R, ..., and so on. The b state, on the other hand, exhibits the sequence of α, β_R, α, β_L, α, β_R, ..., where the α pattern is followed by β_R and β_L alternatively.

Next we consider the chaotic states. Figures 3(e) and 3(f) show the phase portraits corresponding to the chaotic state of Fig. 2(b). Notice that the trajectory in the (4,3) mode keeps coming back near to the point denoted by S. On the other hand, the trajectory in the (7,2) mode keeps visiting near the points, either R or L . So the spatial pattern competition would exhibit the α pattern followed by either β_R or β_L. How are we sure that the competition is completely chaotic? The answer can be found by rearranging the set of data formed by the re-

currence times τ_i between the β pattern excitations, as illustrated in Fig. 2(b). By plotting τ_{i+1} as a function of τ_i, we found that there exists a well defined one-dimensional function f such that $\tau_{i+1} = f(\tau_i), i = 1, 2, 3 \ldots$. Figure 4 shows the resulting functional form of f.

The function f has an unstable fixed point, i.e., the crossing point between the 45° line and the function f itself; the magnitude of the gradient at the crossing point is greater than 1, so it is unstable. Figure 4 also illustrates how to get τ_{i+1} reversely from the functional form of f, once it is given. Starting from the point near the unstable fixed point, (i) move horizontally to the 45° line and then (ii) move vertically to f, and repeat the processes (i) and (ii): Every time f is hit, we read off its vertical axis, i.e., τ_{i+1}, and in this way we can get the time intervals between the excitations of the (7,2) mode.

How can this function f be related to the chaotic pattern competition? Notice that f consists of two separate walls connected at the sharp peak at the middle. We merely point out here that the existence of the nondifferentiable peak of f results from the existence of the saddle point corresponding to the ridge potential. The right-hand wall, as we found, is constructed only when the trajectory in Fig. 3(f) crosses from left to right or from right to left. If the trajectory stays just in one side without crossing to the other side, then only the left wall of the function f is constructed. Since the system excites the β_R (or β_L) pattern when its phase trajectory visits near R (or L) in Fig. 3(f), we can interpret the specific functional form of f in terms of the coherent patterns as follows. If the successive selection of the β pattern, after each excitation of the α pattern, is such that β_R,β_L,β_R,β_L, then the period of such pattern selection is described by the right-hand wall of f, and if the pattern selection is such that β_L,β_L,β_L ..., or β_R,β_R,β_R ..., then such a period of selecting one pattern is described by the left wall of f.

Significantly, in addition to indicating whether it would be β_R or β_L, the function f also tells about when, or how soon, to pick up the next coming β pattern. In other words, it describes how the time intervals τ_i patch up the time axis. Clearly, the function f plays the role of a clock for the system. The gradient of f, however, indicates that no two time intervals are the same, so that the distribution of the time intervals, $\tau_{i+1}, i = 1, 2, 3 \ldots$ is completely random. Furthermore, the time here is not a simple number but a geometric parameter, as indicated by the sharp peak of f. We may thus refer to this clock as a "nonlinear clock" embedded in the system. The significance of this clock is that it dictates, as we found, what the future "chaotic" pattern selection would be.

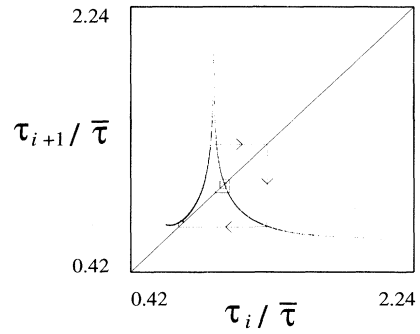

FIG. 4. One-dimensional function f defining $\tau_{i+1} = f(\tau_i), i = 1, 2, 3...$, where τ_i is a time interval between successive excitation of the (7,2) mode, as illustrated in Fig. 2(b). $\bar{\tau}$ denotes the average value of τ_i. The 45° line is inserted for convenience. f has an unstable fixed point, the crossing point with the 45° line. The lines unwinding from the fixed point are inserted to illustrate how to read off τ_{i+1} from f. See the text for the implications of this function f, and for the reasons for calling it a nonlinear clock for the chaotic pattern selection.

Finally, we emphasize that the presence of the same nonlinear clock was actually predicted by the Lorenz chaotic attractor [1,8]. But the physical significance of the clock could not be appreciated by the Lorenz attractor alone. In this respect, the present incidence clearly illustrates its physical implications in terms of coherent patterns, particularly in association with a hydrodynamical system of experimental interest. Furthermore, we found the same clock also embedded in the partial differential equation known as the Ginzburg-Landau equation [8]. These are the evidences supporting, as we believe, the genericity of the clock f in nonlinear systems.

The authors are thankful for the support in part by Korea Atomic Energy Research Institute and in part by Korea Science and Engineering Foundation.

[1] E. N. Lorenz and J. Atmos, Science **20**, 130 (1963).
[2] See, e.g., H. L. Swinney and J. P. Gollub, Phys. Today **31** (8), 41 (1978).
[3] S. Ciliberto and J. P. Gollub, Phys. Rev. Lett. **52**, 922 (1984).
[4] E. Meron and I. Procaccia, Phys. Rev. **34**, 3221 (1986).
[5] M. Faraday, Philos. Trans. R. Soc. London **121**, 299 (1831).
[6] T. B. Benjamin and F. Ursell, Proc. R. Soc. London, Ser. A **225**, 505 (1954).
[7] See, e.g., H. T. Moon, Phys. Rev. Lett. **64**, 412 (1990), and references therein.
[8] H. T. Moon, M. J. Kim, and J. I. Kim (unpublished).